

On the Plastic Flow of Cohesionless Soils

Problèmes du Fluage Plastique des Sols Non-Cohérents

M.V.MALYSHEV Dr.Sc. (Eng.), Professor, Kuibyshev Civil Engineering Inst.,
 YU.K.ZARETSKY Dr.Sc. (Eng.), Laboratory Head,
 YU.E.ZALEZHNEV Cand.Sc. (Eng.), Senior Researcher, Zhuk Hydroproject Research Inst., Moscow, U.S.S.R.

SYNOPSIS Part I (by Zaretsky and Zalezhnev) deals with processes of sub-limiting and super-limiting deformation of fine-grained sand accompanied by dilatancy. Experimental data indicate a limit to shear stress intensity -- the dilatancy limit -- below which the soil is additionally compacted. This limit depends directly on initial density and granulometric composition of the sand. The intensity of shear stress at which failure occurs does not coincide with the dilatancy limit. Laws are given for dilatational compaction and soil loosening, and their agreement with experimental data is analysed. The principal relationships are stated which determine the process of plastic deformation in cohesionless soils throughout the full range of acting stresses, under conditions of a complex stressed state. Part II (by Malyshev) deals with solutions of problems on the stressed state according to Rankine (with zones of active and passive pressure) and according to Prandtl (transient wedge). A plasticity potential is applied for which the state of critical porosity corresponds to an absence of dilatancy. It is shown that the lines usually observed in experimental investigations with the Kurdjumov photographic fixation procedure should be dealt with as envelopes of the paths of particle movement, and not as the slip lines used in the theory of limiting equilibrium of a loose medium.

I. Cohesionless soils are deformed by the action of an external load as the result of rearrangement of the particles with possible failure of some of their number. The process of particle rearrangement of granular materials proceeds during a length of time depending upon the magnitudes of the applied loads. Transition to the stage of failure is to be judged by the stresses at which the rate of shear strains increases sharply and leads to accelerated flow.

Table 1

Particle size, mm :	5-2	2-1	1-0.5	0.5-0.25	0.25-0.1	0.1
Content, % :	0.7	2.1	8.4	36.6	48.4	3.8

An analysis is given below of the results of triaxial tests on a sand (Table 1). Type I tests consist in increasing component σ_1 at $\sigma_2 = \sigma_3 = \text{const}$, and type II tests in decreasing component $\sigma_2 = \sigma_3$ at $\sigma_1 = \text{const}$ (Fig.1). The experimental data are correlated at two values of the relative density: $I_D = 0$ ($\gamma_s = 1.49 \text{ g/cm}^3$) and $I_D = 0.94$ ($\gamma_s = 1.77 \text{ g/cm}^3$).

An examination of the course of shear strain with time in conjunction with the σ_i vs e_i diagrams, where σ_i and e_i are the stress intensity and shear strain, indicates that the failure of cohesionless soils occurs when the intensity of shear strain reaches a definite value

$$e_i = e_i^* \quad (1)$$

In the compact state, the limiting strain

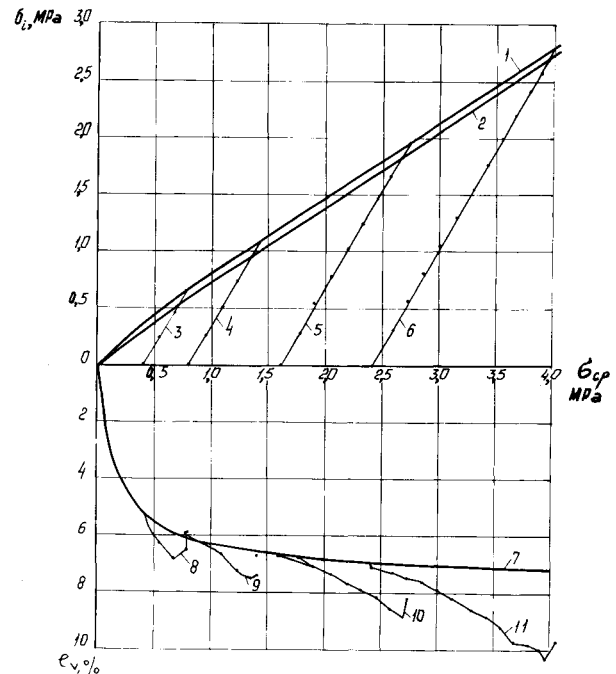


Fig.1. Loading trajectory curves and stress vs volume strain curves: Type I tests at $I_D = 0$ ($\gamma_s = 1.49 \text{ g/cm}^3$)
 1 -- stress at failure; 2 -- dilatancy stress;
 3, 4, 5 -- and 6 -- loading trajectories at initial hydrostatic pressures of 0.4, 0.8, 1.6 and 2.4 MPa, respectively; 7 -- volume strains at the initial hydrostatic pressure; 8, 9, 10 and 11 --

11 - volume strains with deviator loading in tests with initial hydrostatic pressures of 0.4, 0.8, 1.6 and 2.4 MPa, respectively.

at failure depends only slightly on the loading trajectory, while in the limiting loose state, the limiting strain in the type I tests is 1.5 times that of the type II tests. The initial density of the sand has a very substantial effect on the strain at failure (Table 2).

$I_D=0$		$I_D=0.94$	
$\gamma_s=1.49 \text{ g/cm}^3$		$\gamma_s=1.77 \text{ g/cm}^3$	
Type I	Type II	Type I	Type II
$e_i^* = 21 \text{ to } 24\%$	$e_i^* = 16\%$	$e_i^* = 10\%$	$e_i^* = 9 \text{ to } 10\%$

The failure condition can also be stated in terms of the stresses. Since the experiments were conducted only in confined compression test apparatus, the strength criterion was taken in accordance with the Mises-Botkin hypothesis. An examination of various strength criteria and their relationships for different kinds of stressed states is dealt with, for example, by Malyshev (1968). Treatment of the data indicated that the above-mentioned strength criterion is well approximated by the power function

$$\sigma_i^* = f \sigma_m^m \quad (2)$$

where σ_i is the hydrostatic pressure. The exponent $m=0.88-0.89$ turned out to be practically independent of both the initial density of the sand and of the loading trajectory. Factor f depends mainly on the initial density and can be taken the same for the investigated loading trajectories. For the limiting loose state of the sand, this factor equals $f=0.102-0.109 \text{ (MPa)}^{1-m}$ and can be taken equal to $f=0.120-0.133$ for the compact state.

The process of shear deformation of cohesionless soils is accompanied by volume strains. The dilatant portion of the volume strain ($\epsilon_v = \epsilon_v(0) + \epsilon_v(i)$, where $\epsilon_v(0)$ is the volume strain due only to hydrostatic pressure, and $\epsilon_v(i)$ is the volume strain caused by the shear stresses), like the shear strain, proceeds with time. The increment of the dilatant portion of the volume strain may either be positive (additional compaction) or negative (loosening). The value of the shear stress intensity at which the sign of $\Delta \epsilon_v(i)$ is reversed is called the dilatancy stress $\sigma_i^{(d)}$. The conducted experiments show that the dilatancy stress obeys the same relationship that the limiting shear stress does:

$$\sigma_i^d = f_d \cdot \sigma_m^d \quad (2a)$$

The exponent m_d does not depend upon the initial density of the sand and on the loading trajectory ($m_d=0.96 \text{ to } 0.98$), and the parameter $f_d \text{ (MPa)}^{1-m_d}$ depends only on the initial density of the sand and equals $f_d=0.75$ for the limiting loose and $f_d=0.9$ for the limiting compact state. Here the ratio $f_d/f=0.75$ exists.

Progressive flow of sand is always accompanied by its volume loosening ($\Delta \epsilon_v(i) < 0$). In approaching the limiting state and

at $\sigma_i > \sigma_i^{(d)}$, the rate of dilatancy $\lambda = \frac{d \epsilon_v(i)}{d \epsilon_i}$

tends to a constant and, as a rule, negative value λ^* (Fig.2) The limiting value of the

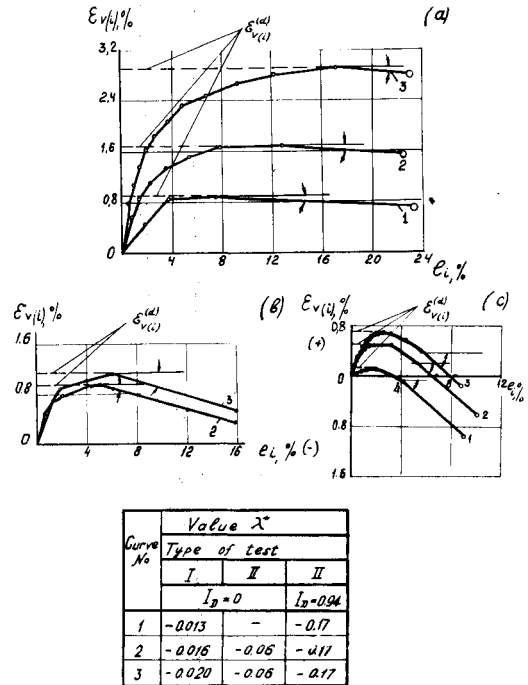


Fig.2 Dependence of the dilatant portion ($\epsilon_v(i)$) of the volume strain on the shear strain intensity (ϵ_i): (a) Type I tests, (b) Type II tests at $I_D=0$; (c) Type II tests, at $I_D=0.94$

rate of dilatancy essentially depends upon the sand density and, to a lesser degree, on the loading trajectory.

The limiting state of a sandy soil with respect to strength is characterized by the same two kinematic conditions:

$$\epsilon_i = \epsilon_i^* \quad \text{and} \quad \lambda = \lambda^* \quad (3)$$

The rate of dilatancy depends upon the shear strain intensity (Fig.4)a and can be expressed in the form

$$\lambda - \lambda^* = \Psi(\epsilon_i) \quad \Psi(\epsilon_i) = n \epsilon_i^n \left(\frac{\epsilon_v(i)}{\epsilon_v(i)^{(d)}} - 1 \right) \quad (4)$$

where $n < 1$.

The strain $\epsilon_v(i)^{(d)}$ corresponds to the maximum value of the positive dilatant portion of the volume strain (Fig.2). The rate of dilatancy can also be expressed as a function of the stress and it obeys a relationship that was established experimentally for entirely different soils (Zaretsky, 1975). This relationship is presented in the form (Fig.3b)

$$\lambda = (\lambda^*) \cdot \frac{\sigma_i^{(d)} - \sigma_i}{\sigma_i^{(d)}} \quad (5)$$

Figure 3c illustrates the checking of equation (5). The limiting value of the rate of dilatancy λ^* , as mentioned above, turned out for sand to be independent of the first in-

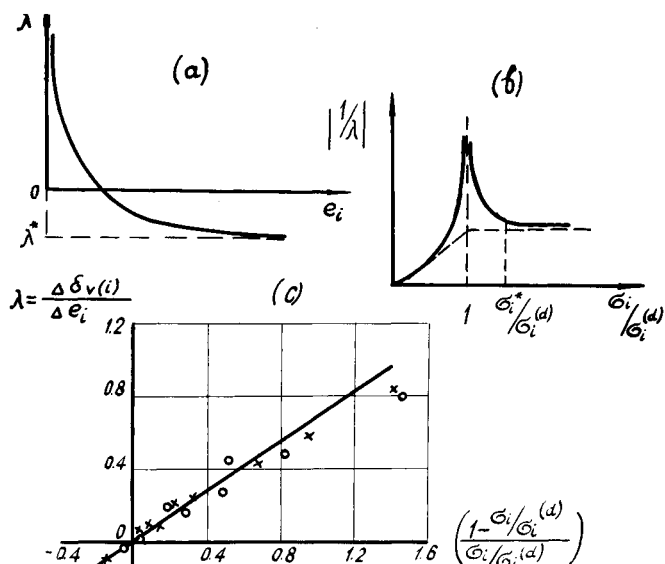


Fig. 3. Dependence of the rate of dilatancy (λ) on the shear stress (σ_i) and the shear strain (e_i): (a) λ vs e_i ; (b) $1/\lambda$ vs $\sigma_i/G_i^{(d)}$; (c) Data of a Type I test at $I_D=0$ ($\gamma_s=1.49$ g/cm³); \circ -- at an initial hydrostatic pressure of 0.8 MPa; \bullet -- ditto, but at 1.6 MPa; \times -- ditto, but at 2.4 MPa

variant of the stress tensor. For cohesive soils (Zaretsky, 1975), the limiting rate of dilatancy decreases with an increase in the sum of the principal stresses. Thus, for cohesionless soils in the sub-limiting state it is possible to apply an incremental theory of plasticity, taking into account holonomic constraints of the type:

$$\left. \begin{aligned} d\epsilon_{ij} &= A_i d\theta_i + A_v d\theta + A_j d\theta_j \\ d\epsilon_{v(i)} &= \lambda d\epsilon_i \end{aligned} \right\} \quad (6)$$

where θ_j is the cube root of the third invariant of the stress deviator, function λ is the rate of dilatancy determined by equation (4) or (5), and A_i, A_v and A_j are functions of invariants of the stress or strain tensor. It should be noted that an experimental confirmation of the coaxiality of the tensors of strain and stress increments and, consequently, of the applicability of an incremental theory of plasticity is given by Roscoe (1970). In applying additional kinematic constraints of the type shown in equations (3) to the limiting and super limiting states, it is evidently necessary to proceed from a statement of the theory of plastic flow that takes these constraints into account.

II. The deformability of soils in states near to the limiting and in the limiting state is often investigated in the laboratory by the photographic fixation method proposed by V.I. Kurdyumov (1961). This method is based on the photography of the soil on a tray and behind a glass wall. As the photograph is being taken, the soil is deformed and the lines produced on the photograph characterize the direction of the displacements. A modification of this method consisted in photography with a movable camera attached to the test plate. (Malyshev, 1953). It is the task of the investigators to interpret the

lines obtained in the experiments. They are frequently identified with the slip lines of the theory of limiting equilibrium of a loose medium (Sokolovsky, 1960). Following Mises, Prager and Drucker (1952) proposed that a plasticity potential be used as a strength condition. The Mohr strength condition can be used for plane and axisymmetric deformation. The theory of limiting equilibrium of a loose medium was developed in conformity with the Mohr strength condition, introducing correction factors φ and C in accordance with the type of stressed state as characterized by the Lode parameter (Malyshev, 1968). From this it follows that soils having friction ($\varphi \neq 0$), have a dilatancy proportional to $\sin \varphi$. It was found in the experiments that the observed dilatancy is less than the theoretical value, and for a soil with critical porosity, according to Casagrande, the dilatancy should equal zero. But the angle of internal friction at critical porosity is not zero, and equals φ^* . It is therefore proposed that the plasticity potential be taken in a form differing from the strength condition (Malyshev, 1971).

$$F = \frac{1}{2} \sqrt{(\sigma_x - \sigma_y)^2 + 4\tau_{xy}^2} - \frac{1}{2} (\sigma_x + \sigma_y) \sin(\varphi - \varphi^*) - c \cot \varphi \sin(\varphi - \varphi^*) \quad (7)$$

i.e. to assume a nonassociated law of plastic flow. The power of mechanical energy dissipation is

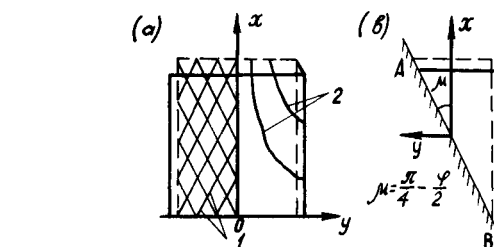
$$D = \lambda [\sin \varphi - \sin(\varphi - \varphi^*)] \cdot [1/2(\sigma_x + \sigma_y) + C \cot \varphi] \quad (8)$$

where λ is the proportionality factor.

The velocity field for the case of a test plate in plane deformation, based on the application of a plasticity potential, was investigated by Shield (1953). Actually, the lines seen on the photograph should be dealt with as the envelopes of vectors of the total displacements of soil particles occurring during the experiment (during photography). If u_x and u_y denote the projections of the displacement vectors, and v_x and v_y , the projections of the velocities of displacement (but not deformation), then, for a plastic rigid body, the path equation is

$$\frac{d_y - d_x}{2\tau_{xy}} = \frac{\partial u_x / \partial x - \partial u_y / \partial y}{\partial u_x / \partial y + \partial u_y / \partial x}; \quad \frac{d_z - d_0}{2\tau_{z0}} = \frac{\partial u_z / \partial z - (\partial u_0 / \partial \theta) / z - u_z / z}{\partial u_0 / \partial z - u_0 / z + (\partial \theta / \partial \theta) / z} \quad (9)$$

The condition for coaxiality of the stress and strain tensors yields



Let us consider the problem of compressing a parallelepiped, using the potential (7), Fig. 4), when $\tau_{xy}=0$ and $\gamma_{xy}=0$. For the boundary

Fig.4. (a) Problem of compressing a parallelepiped in a limiting stressed state: 1-slip lines; 2-paths of displacement; (b) The Rankine problem (the dotted line shows the initial position).

conditions.

(1) $x=H$ and $v_x=v_x^0$; (2) $x=0$ and $v_x=0$; (3) $y=0$ and $v_y=0$ we obtain: $v_x=(v_x^0 x)/H$; $v_y=-v_x^0 \left\{ \frac{1-\sin(\varphi-\varphi^*)}{1+\sin(\varphi-\varphi^*)} y \right\}$ (11)

Integrating equation (9) and applying the condition that the path passes through point $x=x_0, y=y_0$, we have

$$y = \left[\frac{(y_0 x) / x_0}{1 - \sin(\varphi - \varphi^*)} \right] \quad (12)$$

The equation for the slip lines of this problem is $y-y_0=(x-x_0)\tan(\pi/4-\varphi/2)$ (13)

Thus, equation (12) represents a hyperbola, and equation (13), a straight line. The fact that a hyperbola is obtained in the given case follows obviously from the experiment of de Josselin de Jong (1967) using a cube. Dealing, in an analogical statement, with the problem of the motion of a deforming soil massif along a fixed nondeformable rectilinear boundary, coinciding with a slip line and having the equation $dy/dx=\tan\mu$ (required to consider the Rankine passive pressure zone), we obtain (Malyshev, 1971) for a path passing through a point with the coordinates x_0, y_0 :

$$\frac{(x^2+y^2)\cos\varphi-2xy-K(y-x\tan\mu)\cos\varphi}{(x_0^2+y_0^2)\cos\varphi-2x_0y_0-K(y_0-x_0\tan\mu)\cos\varphi} = \frac{(y-x\tan\mu)(y-x_0\tan\mu-K)}{(y_0-x_0\tan\mu)(y-x\tan\mu-K)} \frac{\sin(\varphi-\varphi^*)}{\sin\varphi} \quad (14)$$

$$K = \frac{v_x^0}{\lambda} \cdot \frac{2 \tan\varphi}{\sin(\varphi-\varphi^*)-\sin\varphi}$$

It follows from equations (14) that at $\lambda=0$ (nondeformability) the medium is displaced as a rigid body parallel to itself along AB (Fig. 4b), and at $v_x^0=0$ we have $dy/dx=\tan(\varphi+\mu)$, i.e. the case dealt with by Shield (1953). The angle of emergence of the paths at the surface is determined by quantity K from equations (14). The larger K is, the more gentle the slope at which the paths emerge. The angle of emergence can vary from μ (directions of the velocity vectors and slip lines coincide) to $\varphi+\mu$. If line AB is not fixed with respect to the observer, and is displaced parallel to itself and turns, then the result depends upon the relations between all the velocities of displacement.

In a wedge, when the stress is a power function of the radius, i.e. for the generalized Prandtl problem (Malyshev, 1950):

$$\begin{aligned} \sigma_z &= C z^n (n+m+2) e^{m\theta} - c \cot\varphi; \quad \sigma_\theta = C z^n (n+1)(n+2) e^{m\theta} - c \cot\varphi \\ \tau_{z\theta} &= -C z^n m(n+1) e^{m\theta}; \quad m = \pm \sqrt{4(n+1)\tan^2\varphi - n^2} \end{aligned} \quad (15)$$

The slip lines comprise two families of logarithmic spirals

$$z = z_0 e^{\theta \cot(\omega_0 \pm (\pi/4 - \varphi/2))}; \quad \cos 2\omega_0 = \sin\varphi - \frac{n}{2} \frac{\cos^2\varphi}{\sin\varphi} \quad (16)$$

In the Prandtl case, when the stresses along the radius are constant, $n=0$ and for equation (10) we obtain $(\sigma_r - \sigma_\theta) / 2\tau_{r\theta} = [n(n+2)-m] / [m(n+1)] = \alpha_2$. The velocity components appearing in equation (10) are not the full values but only the deformative ones. The total displacements, including turning of the wedge and the displacement of its poles, are (with respect to the fixed coordinate system of the initial state) equal to

$$\begin{aligned} V_r &= a \cdot \cos\theta - b \sin\theta + C z e^{m\theta} \\ V_\theta &= b \cdot \cos\theta - a \sin\theta + C_r \cdot z + \alpha_2 \cdot C z e^{m\theta} \end{aligned} \quad (17)$$

Hence, the differential equation of the path of displacement is

$$\frac{dz}{z} = \frac{a \cos\theta - b \sin\theta + C \cdot z e^{m\theta}}{b \cos\theta - a \sin\theta + C_r \cdot z + \alpha_2 C \cdot z e^{m\theta}} d\theta \quad (18)$$

where C_r is the angle through which the wedge turns and C is the constant rate of deformation.

REFERENCES

De Josselin de Jong, G. (1967), Free discussion, Proc. of the Geotechnical Conf. Oslo, 1967, Vol. 2, p. 199.
 Kurdyumov, V. I. (1916), A Concise Course of Bases and Foundations, 3rd ed., Erlich Publishing House, Petrograd (in Russian).
 Malyshev, M. V. (1950), Analysis of an Ideally Loose Wedge in a Limiting Stressed State, Doklady USSR Academy of Sciences, vol. 75, Issue 6 (in Russian).
 Malyshev, M. V. (1953), Theoretical and Experimental Investigations of the Bearing Capacity of a Sand Foundation Base, VODGEO Publishers, Moscow (in Russian).
 Malyshev, M. V. and M. D. Fradis (1968), Strength Conditions for Sandy Soils, Acta Technica Academiae Scientiarum Hungaricae, vol. 83, (1-4), p. 167-175, Budapest (in Russian).
 Malyshev, M. V. (1971), On Slip Lines and Paths of Displacement of Particles in a Loose Medium, Jour. Bases, Foundations and Soil Mechanics, No. 6, Moscow, (in Russian).
 Prager, W. and D. C. Drucker (1952), Soil Mechanics and Plastic Analysis or Limit Design, Quart. Appl. Math. vol. 10, No. 2.
 Roscoe, K. H. (1970), The Influence of Strains in Soil Mechanics, Geotechnique, vol. 20, No. 2.
 Shield, R. T. (1963), Mixed Boundary Value Problems in Soil Mechanics, Quart. Appl. Math., vol. 11, No. 1.
 Sokolovsky, V. V. (1960), Statics of a Loose Medium, Gostekhizdat Publishers, 3rd ed. Moscow (in Russian).
 Zaretsky, Yu. K. and S. E. Gorodetsky (1975), Dilatancy of Frozen Soil and the Development of a Deformational Theory of Creep, Jour. Hydrotechnical Construction, No. 2, Moscow (in Russian).